J Mater Sci (2007) 42:4892–4898
DOI 10.1007/s10853-006-0557-y

The effect of N_2 addition upon the MIG welding process of duplex steels

José María Gómez de Salazar · Alicia Soria · María Isabel Barrena

Received: 25 October 2005 / Accepted: 12 June 2006 / Published online: 9 March 2007

Abstract This paper presents the results of a study on the weldability of a duplex stainless steel, Avesta 2205, carried out by GMAW (MIG) pulsed arc welding process. An AISI 2209 electrode (AWS A/SFA 5.9, ER2209) was used as filler metal. The study was focused on the N_2 content in the shield gas, from 0% to 6.4%. Firstly, a microstructural characterization of the welds using scanning electron microscopy (MEB-EDX) was carried out. Also, in order to study the microstructural changes originated by the welding thermal cycles and the % content of the N_2, the ferrite content in the weld pool and heat affected zone (HAZ) were determined. Vickers hardness, tensile and bending tests were performed to determine the mechanical properties of joints and hence the influence of N_2 addition without decrease in the mechanical properties. Finally, the joints were examined for susceptibility to intergranular corrosion using the Standard ASTM 262 93, practice A. The optimal content of N_2 in the shield gas is included between 3% and 5%, which attain to obtain a 94% base material UTS.

J. M. Gómez de Salazar · A. Soria · M. I. Barrena (✉)
Departamento de Ciencia de los Materiales e Ingeniería Metalúrgica, Facultad de Ciencias Químicas, Universidad Complutense de Madrid, 28040 Madrid, Spain
e-mail: ibarrena@quim.sim.ucm.es

J. M. Gómez de Salazar
e-mail: gsalazar@quim.ucm.es

A. Soria
e-mail: asoria@quim.ucm.es

Introduction

Duplex stainless steels present high elastic limits, tensile strength, resistance to pitting corrosion and higher resistance intergranular corrosion than the stainless steels [1]. Due to the alloy's high Cr and low Ni contents, and also to the presence of elements such as Mo, Si (stabilizers the δ—ferrite phase) and V, C, Cu, Mn and N (stabilizers of the γ–austenite phase), the resulting structures exhibit very fine δ (body centre cubic) and γ (face centre cubic) phase structures, whose volume depends on the composition of the alloy and the heat treatment to which it is subjected [2–5].

Welding of duplex stainless steels is a highly developed technique. One of the most common fusion welding procedure is GTAW (Gas Tungsten Arc Welding) with welding energies ranging from 0.5 kJ mm^{-1} to 2.5 J mm^{-1}. An important factor in duplex steel welding is the sensitivity to the cooling gradient [6, 7]. The best properties are achieved with a microstructure consisting of 50% δ and 50% γ and the filler materials must have the same composition than the steel to be welded, or being materials richer in Ni (AISI 2209). Formation of the austenite phase is controlled by diffusion, and therefore it is important to determine the gradient of cooling between 400 °C and 100 °C for a better understanding of nucleation and growth mechanisms from the ferrite phase [8].

Post-welding heat treatments do not improve the austenite content in the weld [9]. However, by increasing the concentration of N_2 in the shield gas, the δ phase can be reduced and the γ phase increased in the melt pool [10, 11]. Addition of N_2 modifies the transformation curves of the Fe_2M and $M_{23}C_6$ phases for longer treatment times, and this enhances the possibility of

chromium nitride (Cr_2N, CrN) formation [12, 13]. Nitrogen likewise affects the kinetics of spinoidal decomposition in the twinning of the Cr-rich δ phase, which can also be reduced by plastic deformation [14].

The microstructure of the melt pool is normally dendritic in fast-cooling zones or globular in slow-cooling areas. This microstructure is largely dominated by nucleate and growth mechanisms of the ferritic or the austenitic phases on ferrite grain limits. Also, secondary austenite produces Widmanstätten structures. Nitrogen is highly soluble in austenite and tends to segregate, and this may reduce precipitation of Cr nitrides [15]. Phases like χ, σ and α' can form in regions with low cooling gradients [16]. A problem associated with the addition of nitrogen to the welding gas is that high nitrogen concentrations (>4%) hinder arc stability (they cause splattering, make for a very erratic welding arc and increase turbulence in the melt) [17].

Experimental procedure

The material used in this research was an Avesta 2205 duplex stainless steel (UNS No. S31803) made by Avesta Sheffield in sheet form. It is rolled to a thickness of 5 mm and treated by solubilization at 1,200 °C. The chemical composition and the mechanical properties of this steel are shown in Tables 1 and 2, respectively.

The duplex stainless steel was welded using MIG procedure. The welds were carried out using a 2209 duplex steel ER2209 (AWS A/SFA 5.9) from ESAB as filler material ($\varnothing_{filler}$ = 1.2 m). The filler composition is shown in Table 3. The welding equipment was an Aristo 500 and the protective gas used was Ar + 2% CO_2 (flow: 13–16 L min^{-1}) with addition of N_2. The joints were single V-groove types at 70°.

To determine the effect of the N_2 addition upon the welded duplex steels a microstructural and mechanical evaluation of these materials were carried out. In order to find the welding and filling rate optimal parameters a high amount of welds were carried out. Welding and filling rate were fixed as 30 cm min^{-1} and 7 m min^{-1}, respectively. Table 4 shows the welding parameters used for the four conditions tested. The content % of N_2, in the shield gas were modified from 0% to 6.4%. Standard (UNE-EN 288) 300 × 150 mm plates were placed on the welding bench on a copper backing. Welding was performed by a automated apparatus (BUGO^{TM}).

Base material and welds were examined to determine microstructure, the δ (ferrite phase) content and the mechanical properties of the weld (hardness, tensile and bending tests according to UNE-EN 1043-1, ASTM A370 and UNE-EN 910, respectively).

Scanning electron microscopy (SEM-EDX) studies were performed on the transverse axis of the welds using a JEOL 6400 (SEM) linked to an EDX microanalyser. Metallographic specimens were cut and embedded in a polyester resin, grinded, polished and etched on the transverse axis of the welds.

Microhardness testing of the base material was made in the three directions, L-longitudinal direction, LT-large transversal direction and ST-short transversal direction. Welds microhardness profiles were conduced on a cross-section of transverse specimens from melt pool to base material (without thermal effect). The measurements were performed by Vickers indentation (UNE 7-423-84), using an Akashi MVK-A3 microhardness with a 100 g indentation load.

The ferrite content of the material was determined using a Fisher MMS-3-AM ferritoscope. The analyses were carried out on the polished surfaces without etching.

Table 1 Chemical composition of Avesta 2205 (wt%)

Element	C	Cr	Ni	Mo	N	Mn	Si	S	P
wt%	0.017	21.82	5.72	3.01	0.155	1.51	0.34	0.001	0.022

Table 2 Properties of Avesta 2205

Mechanical property	Maximum value
Yield strength (MPa)	480 ± 10
Tensile strength (MPa)	780 ± 15
Hardness ($HV_{1\ kg}$)	250 ± 5
Elongation (%)	>25%

Table 3 Chemical composition of filler AWS A/SFA 5.9 (wt%)

Element	C	Cr	Ni	Mo	N	Mn	Si	S	P
wt%	0.02	22.5	9.5	3.1	0.14	0.9	0.9	0.001	0.022

Table 4 Experimental welding conditions

Condition	Weld A	Weld B	Weld C	Weld D
Gas flow (L min^{-1})	16	14.84	14.26	13.67
% (Ar + 2% CO_2)	100	97.04	95.37	93.63
% N_2	0	2.96	4.83	6.4
Mean voltage (V)	26.06	26.36	26.56	27.25
Mean current (A)	179.3	175.3	177.5	163.3
Energy (kJ mm^{-1})	0.935	0.924	0.943	0.890
Welding rate V_s (cm min^{-1})	30	30	30	30
Filling rate V_f (m min^{-1})	7	7	7	7
Electrode distance (mm)	15	15	15	15
Separation (mm)	1.80	1.80	1.80	1.80

Mechanical tests (tensile and bending tests) were performed for all welds to determine the relationship between the properties and the microstructural changes originate by welding thermal cycle, using a universal testing equipment (10 Tn) Servosis MEM-10.

Susceptibility to intergranular corrosion was also tested in accordance with Standard ASTM 262-93, practice A. The probes were etched by immersion in electrolytic oxalic acid (10%) with a current density of 1 A cm^{-2} for 1.5 min. Surfaces were then examined by optical microscopy at 500 magnifications.

Results and discussion

The microstructure of the duplex stainless steel, Avesta 2205 (Fig. 1) is typical of a duplex rolled steel, showing alternating grains of δ ferrite in dark and austenite (γ phase) in white, elongated in rolling direction. The EDX microanalyses of δ and γ phases marked in Fig. 1 show the composition of both phases in the as-received material. In the solid solutions (γ phase) there are isolated titanium microinclusions randomly distributed in the matrix. Figure 2 shows the SEM image and the EDX microanalysis of titanium nitride inclusions on ferrite to check the matrix effect of analysis.

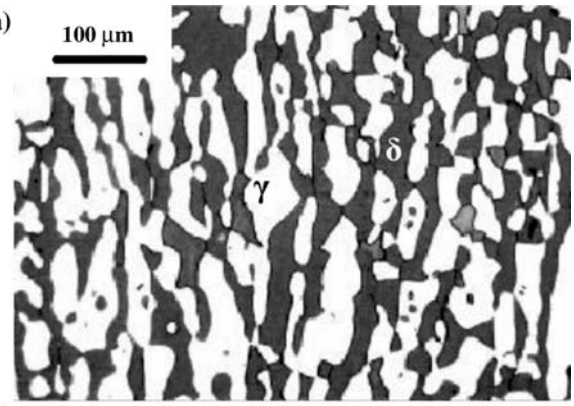

(b)

Element (γ phase)	Weight%	Atomic%
Cr K_α	22.66	20.28
Fe K_α	63.41	52.85
Ni K_α	5.20	4.12
Element (δ phase)	**Weight%**	**Atomic%**
Cr K_α	24.06	23.02
Fe K_α	64.16	57.14
Ni K_α	4.87	4.12

Fig. 1 (**a**) Microstructure of the Duplex Steel Avesta 2205, where γ and δ phases present different metallographic attack. (**b**) The EDX microanalyses of both phases show the composition in the material

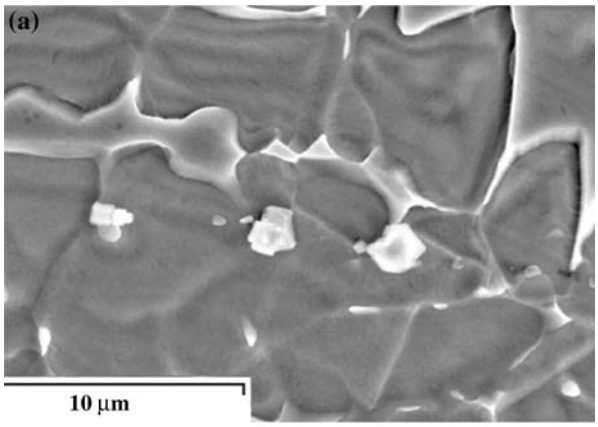

(b)

Element	Weight%	Atomic%
N (K_α)	38.71	69.87
Ti (K_α)	26.38	13.92
V (K_α)	1.52	0.75
Cr (K_α)	15.21	7.40
Fe (K_α)	15.96	7.22
Ni (K_α)	1.54	0.66
Mo (L_α)	0.68	0.18

Fig. 2 (**a**) SEM image and (**b**) the EDX microanalysis of titanium nitride inclusions on ferritic phase

Figure 3 shows transverse metallographic sections from each of the four experimental beads (A–D). Vickers hardness profiles are marked in all figures. The melts pool shows typical columnar grain structures, with an increasing of content of secondary γ phase from bead A to bead D (Fig. 4) with increasing N_2 content. The secondary γ phase is associated with lower hardness values than primary γ phase. When the concentration of N_2 in the welding gas was raised, there was more splattering and the arc became more unstable (Fig. 5). The secondary γ phase of the joints have a higher Ni content than the base material but lower than the Ni content in the filler material, due to a dilution process which take place during welding process.

In order to know the effect of N_2 addition in the welds, the δ content and hardness values obtained in the base material and the welded material were measured (Table 5). Figure 6 shows the results of ferritometry obtained in all welds. Ferrite content in the melt pool decreased from approximately 45% in weld A (0% N_2) to 33% in weld D (6.4% N_2), which proves the stabilizing effect of N_2 addition in the γ phase. These results allow obtaining an equation to calculate the ferrite content in the melt pool as a function of the amount of nitrogen in the welding gas:

$$\delta(\%) = 44.74976 - 1.87306 \cdot N_2(\%)$$

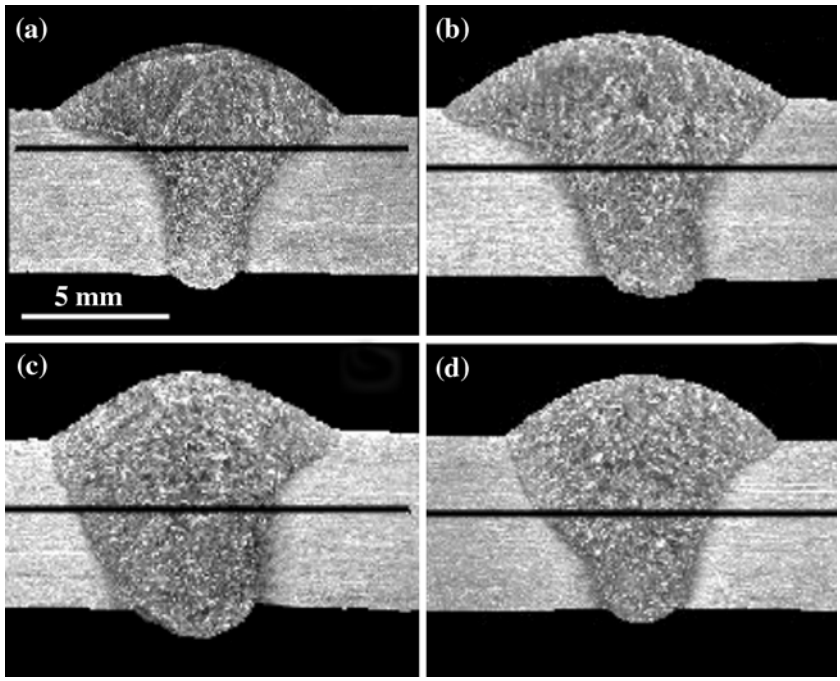

Fig. 3 Image of the transverse section in four MIG joints duplex steel (**a**) weld A (0% N_2); (**b**) weld B (2.96% N_2); (**c**) weld C (4.83% N_2) and (**d**) weld D (6.4% N_2)

The heat-affected zones (HAZ) were very narrow in all welds. These zones contain ferrite (between 40% and 42%) and primary and secondary austenite (between 58% and 60%). Ferrite grains in the surroundings of the melt pool tended to recrystallize and grow, thus becoming less elongated and more equiaxial.

Chromium nitrides were not observed, however this phase exists in the welds but their sizes are very small. This fact could be deduced since the austenite phase (γ) is not as hard as the ferritic phase (δ), and therefore an increase in austenite content substantially reduces hardness in the melt pool. Cr nitride could be the response to increase hardness values in the melt pool over the metal base hardness values. Figure 7 shows the hardness profiles of the four welds. In this figure, low hardness values of the HAZ are observed, which are associated with a high content of the secondary γ phase and recrystallized δ phase.

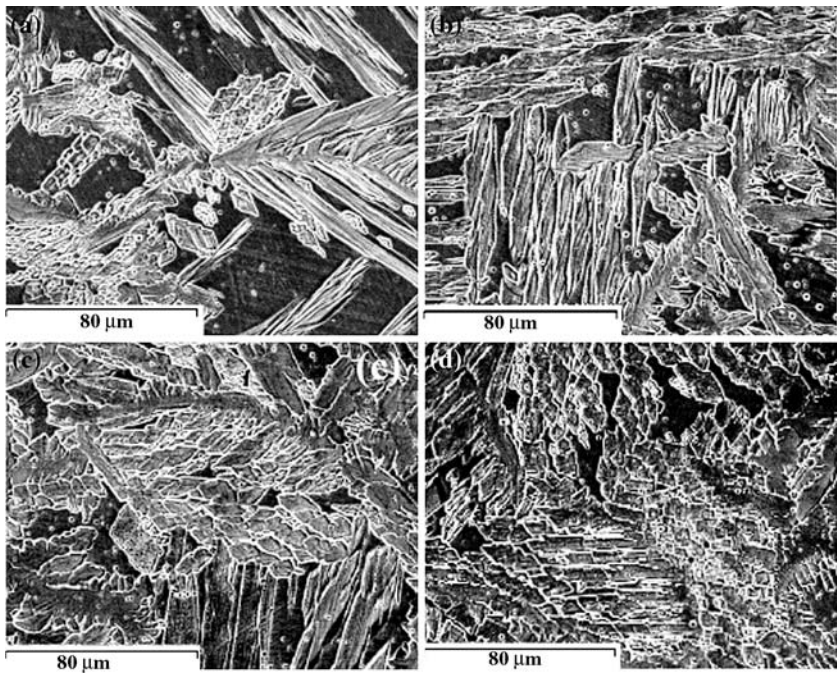

Fig. 4 The effect of N_2 addition to the γ phase content observed in the melt pool of four MIG joints duplex steel (**a**) weld A (0% N_2); (**b**) weld B (2.96% N_2); (**c**) weld C (4.83% N_2) and (**d**) weld D (6.4% N_2)

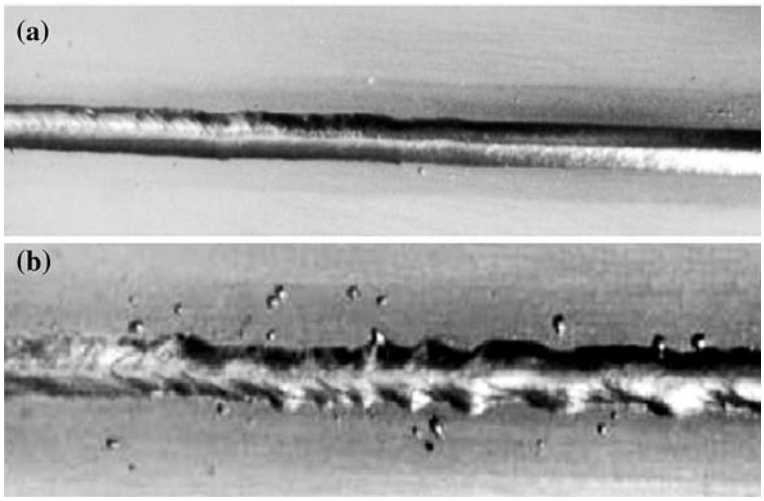

Fig. 5 Macrograph joint longitudinal section of the weld (**a**) weld B (2.96% N_2) and (**b**) weld D (6.4% N_2)

Table 5 Hardness and ferrite content of base material (Avesta 2205)

		Direction (L)	Direction (TL)	Direction (TC)
Hardness ($HV_{1\ kg}$)	Mean	253.6	246.6	245.8
	Standard deviation	7.5	2.8	2.1
% Ferrite	Mean	41.8	38.6	39.4
	Standard deviation	0.9	0.8	2.8

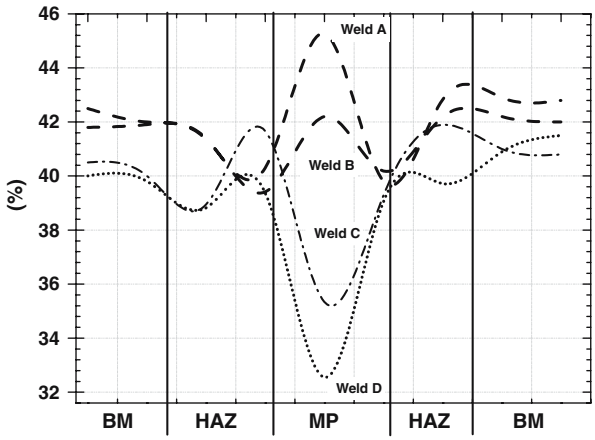

Fig. 6 Ferrite percentage profiles on welded duplex steels

Tensile and bending tests of welds concluded that the welds were between standard limits. Table 6 shows the tensile strength results. The welds ultimate tensile strength (UTS) are higher than 90% of base material UTS. Therefore, the N_2 addition does not provoke important loss in the mechanical resistance of the weld material. Moreover, the thermal cycle of the weld process origin a decrease in the elongation values. However, when the N_2 is added in the welding gas, this property decreased in a lower degree. The A welding condition (0% N_2) generates a low deformation grade (9%). When the N_2 content is increased (between 3% and 5%) the γ phase content is high, decreasing therefore the hardness values and increasing the toughness. In these cases, the fracture occurs in base material. However, when the N_2 content is up to 5%, two effects are combined: higher content of secondary γ phase and the appearance of brittle phases, such as CrN or Cr_2N with small size. This fact provokes that the UTS and elongation values decrease and the fracture mechanism takes place by the fusion line. The bending tests did not provoke cracking in any welds, which indicates high quality welds. These results are illustrated in Fig. 8, which shows two macrographs of a bending test, both face (Fig. 8a) and root (Fig. 8b). Mechanical results confirm that big size nitride phase is not present in the welds.

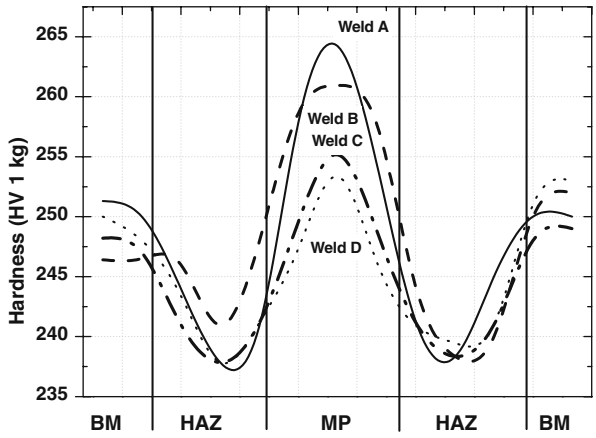

Fig. 7 Hardness profiles on welded duplex steels

Table 6 Tensile test results

Weld	EBA(J mm^{-1})	ENA(J mm^{-1})	Ultimate tensile strength (UTS) (MPa)	Weld UTS as % of base material UTS	ε (%)	Location of fracture
A	936	655	730	94	9.30	Fusion line
B	925	648	730	94	18.06	Base metal
C	939	658	719	92	17.68	Base metal
D	892	624	694	89	15.42	Fusion line

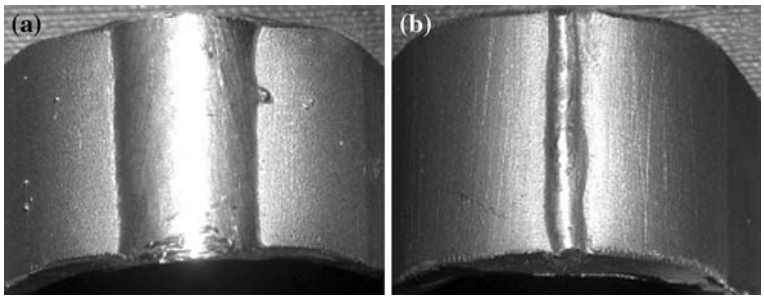

Fig. 8 Typical sample after suffering bending test (**a**) face of weld and (**b**) root of weld

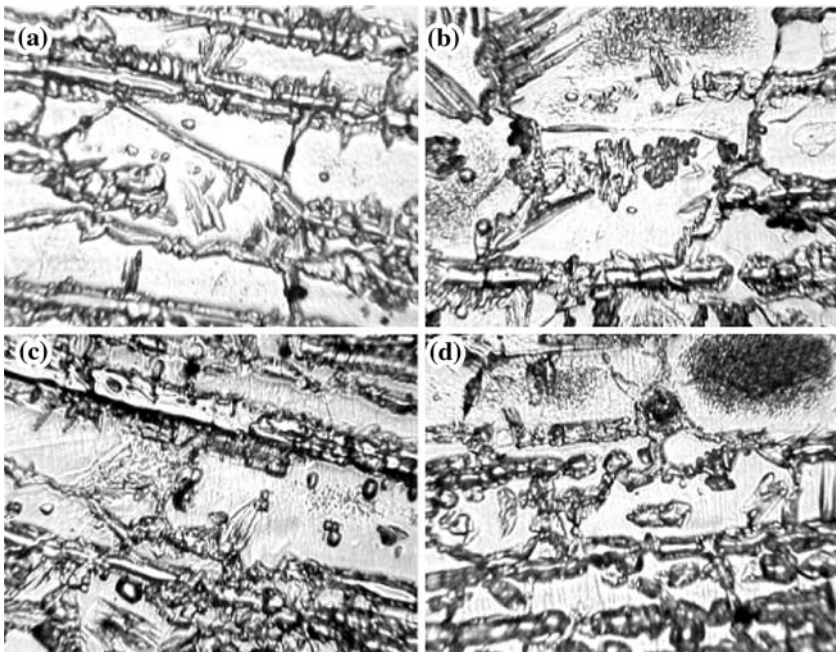

Fig. 9 Optical image (magnification: ×500) of attack surface in the HAZ (**a**) weld A (0% N_2); (**b**) weld B (2.96% N_2); (**c**) weld C (4.83% N_2) and (**d**) weld D (6.4% N_2)

Examination of welds A–D by Standard ASTM 26293-Practice A, showed very good performance in all four welds. No intergranular or interdendritic ditches were found. Some pits were randomly observed. All four welds, then, performed excellently with regards to susceptibility to intergranular corrosion. Figure 9 shows a photographic composition of the results of the ASTM test in HAZs. This corrosion behaviour will allow to carry out this welding type in duplex steel used to manufacture corrosive gas or liquid containers.

Conclusions

The investigation on the effect of N_2 addition upon the MIG welding process of duplex steels allowed drawing the following conclusions.

1. Avesta 2205 duplex steel was welded by MIG pulsed arc with ER 2209 filler. The welding gas was Ar with N_2 added up to 6.4%, 2% higher than previous investigations.

2. The ferrite content in the welds was determined and used to deduce a correlation with the percentage of nitrogen in the welding gas.
3. No phases such as CrN, Cr_2N, σ or other intermetallic compounds were detected either in the melt pool or the HAZ. This fact confirms that the design and the parameter of the welding are suitable for this material.
4. The welding thermal cycles (0% N_2 in shield gas) provokes reduction of the UTS and the elongation values of the welded material. The N_2 addition in the welding gas, from 0% to 5% allows increasing the elongation values of the welds, the UTS welds up 90% UTS base material and additionally the susceptibility to intergranular corrosion is not observed in all welds.

Acknowledgements The author's wish to thank the financial support provided by the project MAT 03-05004.

References

1. Nilsson JO, Karlosson L, Anderson JO (1995) Mater Sci Tech 11(3):276
2. Kuwana T, Kokawa H, Tsujii H (1986) Trans Jap Weld Soc 1**7**(1):15
3. Mateo A, Gironès A, Keichel J, Llanes L, Akdut N, Anglada M (2001) Mater Sci Eng A 314:176
4. Smith J, Farror RA (1993) Inter Mater Rev 38(1):21
5. Johansson KA (1994) Duplex stainless steel in offshore applications, Proceeding of the Conference Duplex. 94:86
6. Pathak K, Datta GL (2005) Sci Technol Weld Joi 10(2):139
7. Petterson O, Demestres JM (2001) Sold Tecn Unión 68:9
8. David SA, Vitek JM (1989) Inter Mater Rev 34(5):213
9. Mahmoud SM (1997) Transformaciones debidas a ciclos térmicos de soldadura y tratamientos térmicos del acero inoxidable SAF2205. PhD Thesis, Universidad Complutense de Madrid
10. Li X (1997) Production and assessment of microstructures in a duplex stainless steels. Ph.D. Thesis, University of Birmingham
11. Capello E, Chiarello P, Previatali B, Vedani M (2003) Mater Sci Eng A 351:334
12. Glownia J, Kalandyk B, Hübner K (2001) Mater Char 4**7**:149
13. Ramirez J, Brandi SD, Lippold JC (2004) Sci Technol Weld Joi 9(4):301
14. Weber L, Uggowitzer RJ (1998) Mater Sci Eng A 242:222
15. Polak J, Fardoun F, Degallaix S (2001) Mater Sci Eng A 297:154
16. Cortie MB, Jackson EM (1997) Metall Mater Trans A 28:2477
17. Zhao L, Lugscheider E, Fischer A, Reimann A (2001) Surf Coat Techn 141:208